



Published in final edited form as:

Pain. 2022 January 01; 163(1): e106–e120. doi:10.1097/j.pain.0000000000002321.

Sympathectomy decreases pain behaviors and nerve regeneration by downregulating monocyte chemokine CCL2 in dorsal root ganglia in the rat tibial nerve crush model

Xiaoyan Zhu^{a,b,*}, Wenrui Xie^a, Jingdong Zhang^a, Judith A. Strong^a, Jun-Ming Zhang^a

^aPain Research Center, Department of Anesthesiology, University of Cincinnati College of Medicine, Cincinnati, OH 45267, U.S.A.

^bDepartment of Anesthesiology, Xiangya Hospital, Central South University, Changsha, Hunan 410008, China.

Abstract

Peripheral nerve regeneration is associated with pain in several preclinical models of neuropathic pain. Some neuropathic pain conditions and preclinical neuropathic pain behaviors are improved by sympathetic blockade. In this study we examined the effect of a localized “microsympathectomy,” i.e., cutting the gray rami containing sympathetic postganglionic axons where they enter the L4 and L5 spinal nerves, which is more analogous to clinically used sympathetic blockade compared to chemical or surgical sympathectomy. We also examined manipulations of CCL2 (monocyte chemoattractant protein 1; MCP-1), a key player in both regeneration and pain. We used rat tibial nerve crush as a neuropathic pain model in which peripheral nerve regeneration can occur successfully. CCL2 in the sensory ganglia was increased by tibial nerve crush and reduced by microsympathectomy. Microsympathectomy and localized siRNA-mediated knockdown of CCL2 in the lumbar DRG had very similar effects: partial improvement of mechanical hypersensitivity and guarding behavior; reduction of regeneration markers growth-associated protein 43 (GAP43) and activating transcription factor 3 (ATF3); and reduction of macrophage density in the sensory ganglia and regenerating nerve. Microsympathectomy reduced functional regeneration as measured by myelinated action potential propagation through the injury site and denervation-induced atrophy of the tibial-innervated gastrocnemius muscle at day 10. Microsympathectomy plus CCL2 knockdown had behavioral effects similar to microsympathectomy alone. The results show that local sympathetic effects on neuropathic pain may be mediated in large part by the effects on expression of CCL2, which in turn regulates the regeneration process.

Introduction

Peripheral nerves can regenerate and reinnervate their target tissues. This process is often studied in rodents using crush or transection of the entire sciatic nerve. In contrast, many

Correspondence to: Jun-Ming Zhang, M.D., M.Sc., Pain Research Center, Department of Anesthesiology, University of Cincinnati College of Medicine, 231 Albert Sabin Way, Cincinnati, OH 45267-0531, Phone: +1-513-558-2427, Fax: +1-513-558-0995, Jun-Ming.Zhang@uc.edu.

*Present address

rodent models of neuropathic pain use partial sciatic nerve injuries, so that pain behaviors related to the hindpaw region can still be studied. We previously demonstrated that the regeneration process was linked to pain behaviors in the rat spared nerve injury (SNI) model of neuropathic pain⁶², in which two branches of the sciatic nerve are ligated and transected. In this model the peripheral regeneration process cannot lead to successful reinnervation, and instead results in neuroma formation. We found that interfering with the regeneration process reduced mechanical and cold hypersensitivity, as well as paw guarding behavior. Peripheral nerve regeneration is associated with pain in several other preclinical models^{14,33,51,67}. A human study of diabetic neuropathy⁷ also showed an association between pain and expression of the nerve regeneration marker growth associated protein 43 (GAP43).

Some pain conditions are maintained or exacerbated by sympathetic nervous system activity, possibly occurring via direct effects of sympathetic transmitters on sensory neurons (especially in pathological conditions where sympathetic sprouting occurs), and via sympathetic effects on immune function⁵³. In immune organs sympathetic innervation is often anti-inflammatory, but local effects in other tissues may be pro-inflammatory^{18,44,53}. We previously described a localized method of sympathectomy, termed “microsympathectomy” (mSYMPX): the grey rami carrying postganglionic sympathetic fibers are transected near their entry to the spinal nerves near the L4 and L5 DRG in rats. In a rat pain model induced by locally inflaming the L5 DRG, mSYMPX markedly reduced both pain behaviors and type I inflammation⁶⁰ (i.e., classical inflammation that involves tissue destruction, nitric oxide, reactive oxygen species, M1 polarized macrophages and Th1 T cells^{2,46}). More recently, we showed that mSYMPX reduced regeneration processes in the SNI model⁶³. In the present study, we examined the relationship between sympathetic nerves, pain, and regeneration in a modified version of this model, in which the tibial nerve was crushed rather than being ligated and transected. As reported by the original developers of this model¹⁵, simply crushing the nerve results in a shorter duration of pain behaviors, as the regeneration process can more readily be completed.

Here we report that mSYMPX reduces pain behaviors and measures of inflammation and regeneration following tibial nerve crush. One molecule that was upregulated by nerve crush and downregulated by mSYMPX was CCL2 (monocyte chemoattractant protein 1 /MCP1). CCL2 upregulation in DRG neurons after peripheral nerve injury has previously been shown to play a key role in both macrophage infiltration into the DRG and the nerve regeneration response⁶⁸. It has also been previously implicated in neuropathic pain⁶. We found that knocking down CCL2 expression in the DRG could mimic many of the behavioral and biochemical effects of mSYMPX in the tibial crush model.

Methods:

Animals:

The experimental protocol was approved by the University of Cincinnati Institutional Animal Care and Use Committee. Experiments were conducted in accordance with the National Institute of Health Guide for the Care and Use of Laboratory Animals. Adult

Sprague Dawley rats of both sexes (Envigo, Indianapolis, IN) weighing 80 – 100 grams were used in approximately equal numbers. In the figures, data from both sexes have been combined; figures with male and female behavioral data shown separately are available as supplemental data.

Surgical procedure for tibial nerve crush:

The procedure for the tibial nerve crush was modified from the previously described SNI model in which the tibial and common peroneal nerves are ligated and sectioned¹⁵; these authors also reported on effects of simply crushing these nerves using methods similar to those adopted here. The skin on the lateral surface of the right thigh was incised and blunt dissection through the biceps femoris muscle exposed the sciatic nerve and its three terminal branches: the sural, common peroneal and tibial nerves. After cleaning off the connective tissue, the tibial nerve was crushed ~2–3 mm distal to the trifurcation for 30 s by a small arterial microclip (0.8mm wide x 5 mm long, catalog number RS-5420, held with microclip-applying forceps, catalog RS-5440, Roboz, Gaithersburg, MD) with smooth protective pads formed by silicon tubing placed over the blades. At the end of this procedure the tibial nerve was completely flattened and transparent. The incision was closed in layers.

Surgical procedure for microsympathectomy (“mSYMPX”):

Cutting of the grey rami was performed as in our previous study⁶⁰. Briefly, just prior to implementing the nerve crush, the proximal L4 and L5 spinal nerves and transverse processes were exposed. The gray rami entering the L4 and L5 spinal nerves close to the DRGs (i.e. coming from the L3 and L4 sympathetic paravertebral ganglia according to the nomenclature of Baron⁴) were dissected away from nearby blood vessels and cut near their entry point into the spinal nerve. Around 1 mm of gray ramus was further removed to make a gap and slow regeneration. Sham controls received similar exposure of the spinal nerves but the gray rami were not cut. We have previously shown that the mSYMPX procedure causes loss of sympathetic fibers in the DRG and surrounding capsule, as well as in the hindpaw, using immunohistochemical staining for tyrosine hydroxylase 7 days after mSYMPX, and did not show recovery at 28 days⁶⁰

Surgical procedure for injecting siRNA into lumbar DRGs:

siRNAs directed against rat CCL2 (NCBI gene ID 24770) and nontargeting control were designed by and purchased from Dharmacon/ThermoFisher (Lafayette, CO) as in our previous studies. The siRNA was siGENOME™ siRNA consisting of a “smartpool” of four different siRNA constructs combined into one reagent, catalog number M-080146–01 (CCL2) and D-001210–02 (nontargeting control directed against firefly luciferase, screened to have minimal off-target effects and least 4 mismatches with all known human, mouse and rat genes according to the manufacturer). The sequences of the CCL2 siRNA were: GAACUUGACCCAUAAAUCU, UGAGUCGGCUGGAGAACUA, GAUCAGAAACUACAGUCUU, and GCUAAUGCAUCCACUCUCU. During the mSYMPX surgery, just prior to transection of the grey rami, 3 µL aliquots containing 80 pmoles of siRNA made up with cationic linear polyethylenimine (PEI)-based transfection reagent (“in vivo JetPEI”, Polyplus Transfection, distributed by VWR Scientific, USA) were injected into the L5 and L4 DRGs, through a small glass needle (75 µm o.d.) inserted

close to the DRG through a small hole cut into the overlying membrane close to the site where the dorsal ramus exits the spinal nerve, as previously described⁶¹. The injections were performed just prior to tibial nerve crush, in a single surgery.

Procedures for measuring functional regeneration:

In vivo fiber recording methods were used to estimate the degree of functional regeneration of myelinated axons through the tibial crush site. On day 10 after tibial crush plus mSYMPX or sham mSYMPX, rats were anesthetized with pentobarbital (40 mg/kg) with additional boluses of i.v. pentobarbital as needed. The tibial nerve was exposed around the injury site and the sciatic nerve was exposed more proximally, near its origins in the junction of the L4- L6 spinal nerves. At both sites skin flaps were used to form pools filled with warm light mineral oil for placement of the electrodes. A silver wire ~1mm in diameter was inserted into the sciatic nerve transversely to serve as the recording electrode. A bipolar stimulating cuff electrode was placed distal to the crush site and compound action potentials were elicited with 0.5 and 1.0 mA, 1.0 msec stimuli. The stimulating electrode was then moved to a tibial nerve site proximal to the crush site and the stimuli repeated. The fast peak (A- α and A- β fiber) of the compound action potential was measured (average value from 3 stimuli per condition) and the ratio of distal to proximal amplitude was used as a measure of the fraction of fibers that failed to functionally regenerate (i.e., including remyelination and normalization of threshold as well as any required regrowth through the injury, of both sensory and motor fibers) through the crush site. In some animals additional peaks could be observed after the main peak, presumably due to fibers with incomplete recovery of the conduction velocity, however, adding these peaks to the primary peak did not change the experimental conclusions. We relied on the mineral oil to isolate the tibial nerve from surrounding nerves, but cannot completely rule out some contribution to the CAP from nearby nerve branches. At the end of the experiment the gastrocnemius muscle (both medial and lateral) was removed on both sides as described in³⁶, the wet weights obtained, and the ratio of the ipsilateral to contralateral muscle used as a measure of denervation-induced muscle atrophy.

Behavior testing:

Static mechanical sensitivity was tested by applying a series of von Frey filaments to the lateral heel region of the paws, using the up-and-down method⁹. This test site in the sural nerve territory was selected so that hypersensitivity could be measured from early time points after the tibial crush^{3,15}. A cutoff value of 15 grams was assigned to animals that did not respond to the highest filament strength used. A wisp of cotton pulled up from, but still attached to a cotton swab was stroked mediolaterally across the plantar surface of the hindpaws to score the presence or absence of a brisk withdrawal response to a normally innocuous mechanical stimulus (dynamic tactile allodynia). This stimulus does not evoke a response in normal animals. Cold sensitivity was scored as withdrawal responses to a drop of acetone applied to the ventral surface of the hind paw. When observed, responses to acetone or light brush strokes consisted of several rapid flicks of the paw and/or licking and shaking of the paw; walking movements were not scored as positive responses. The stimuli for the dynamic tactile allodynia and cold allodynia tests spread over a wider region than the von Frey test and included regions outside the tibial territory. Spontaneous guarding

behavior was scored⁶⁵ as 0 (no guarding, paw flat on floor), 1 (mild shift of weight away from paw), 2 (unequal weight bearing and some part of the foot not touching the floor), or 3 (foot totally raised or not bearing any weight); these scores were recorded just before each application of the von Frey filament (6 observations per paw total) and averaged.

Microscopy:

Four days after tibial crush (with or without other manipulations as indicated), animals were anesthetized with 1% pentobarbital sodium i.p., perfused with 0.1M phosphate buffer until clear fluid was seen, then perfused with 4% paraformaldehyde for 20 minutes. For immunohistochemistry, tibial nerve cross sections or L4/L5 DRG sections were cut at 12 μm , while tibial nerve longitudinal sections were cut at 40 μm , on a cryostat after post fixation in 4% paraformaldehyde, 0.1M Phosphate Buffer, 3% sucrose. The sections were blocked with 10% serum for 1 h and then incubated with primary antibodies at 4°C overnight. Afterwards, the sections were incubated with secondary antibodies 2 h at room temperature. Negative controls lacked the primary antibody. After the incubation, sections were washed with PBS (0.01 M, pH 7.4) three times for 10 min. The following antibodies were used for the indicated targets: CCL2 antibody (rabbit, 1:1000; Novus NBP1– 07035 polyclonal, RRID:AB_1625612); growth-associated protein 43 (GAP43) antibody (rabbit; 1:500; Abcam Catalog ab16053, RRID: AB_443303), a marker for nerve regeneration; Iba-1 antibody (goat, 1:500; Abcam, catalog ab5076, RRID: AB_2224402), a general marker for macrophages and microglia^{25,26,28}; NeuN antibody, neuronal marker, (Abcam ab104224 mouse monoclonal, 1:1000, RRID: AB_10711040); and activating transcription factor 3 (ATF3; Novus NBP1–85816 rabbit polyclonal, 1:100, RRID:AB_11014863). We have previously validated the GAP43 antibody by demonstrating decreased staining after siRNA-mediated knockdown in the DRG following spinal nerve ligation –induced upregulation⁶². We previously validated the Iba-1 antibody by showing loss of signal when the antibody was pre-absorbed with the immunizing antigen (Abcam catalog ab23067, used at 20-fold molar excess) and showing lack of coexpression with markers for DRG satellite glia cells, in DRG neurons, or in most cell types present in uninjured peripheral nerve⁶³. In this study we show that siRNA directed against CCL2 mRNA reduces staining by the CCL2 antibody. This consistency provides evidence for the specificity of these independent methods of investigating CCL2, since non-specific off-target effects would be expected to differ between the two methods. (None of the siRNA constructs target the portion of the reference mRNA, Reference Sequence: NM_031530.1, that encodes the portion of the protein used as the antigen to create the antibody). As further confirmation of this antibody, we confirmed the upregulation of CCL2 in DRG and nerve by tibial crush observed in the immunohistochemical experiments, by using an Elisa kit (Invitrogen/ThermoFisher, catalog BMS631INST) according to the manufacturer's instructions; in DRG CCL2 concentration increased from 6.9 ± 1.2 in normal and sham operated rats to 18.7 ± 1.6 pg/ml, ($p < 0.001$, t test); in tibial nerve from 1.6 ± 1.0 to 59.9 ± 7.2 , $p < 0.001$, test; $n = 7-8$ rats/group). The ATF3 antibody showed the previously reported DRG expression pattern (neuronal nuclei) observed after peripheral nerve injury^{24,56}, with low expression in normal DRG, and has been validated by demonstration of nuclear signal in axotomized DRG neurons in normal but not Cre-mediated ATF3 conditional knockout mice²².

In some experiments, two primary antibodies were used for each section, in order to examine two targets at once. In general this was done to obtain more information from a given animal, not to demonstrate co-localization, so in some cases the results from the two antibodies are presented in two different figures. In some cases the color of the secondary antibody was transformed after image acquisition to maintain constant colors for a given antigen.

For quantification of antibody staining, images from 2 – 5 sections of each DRG or nerve segment, selected at random, were captured using an Olympus BX63F with an LED light source using cellSens Dimensions software, and intensity of signal in each channel was summed over the selected area and normalized by the area measured. For DRG sections, only regions containing predominantly neuronal cell bodies were selected for analysis. When analyzing nerve sections quantitatively, only regions containing fibers were selected and analyzed; the staining in the surrounding nerve sheath was not included in the summed intensities. Signal intensity of the DRG neuronal areas or nerve was measured using Olympus cellSens Dimension Desktop (Olympus Corp., USA). Background levels were determined using negative control from tissue sections incubated in the same secondary antibody but without primary antibody. Image background was then corrected/subtracted by manually adjusting the left and right scaling of the image histograms in cellSens. The same values of the fixed scaling were applied to all the images in the experiment. For quantification of immunohistochemical staining, all image capture and analysis sessions were performed comparing samples from all experimental groups relevant to each experiment, prepared at the same time with the same staining solutions, including samples from all experimental groups on each slide. The images of the slides were then captured and analyzed all in one imaging session, using identical parameters in a side-by-side design. The microscope used exhibited enough stability that the acquisition parameters were kept the same for all the samples in the study.

Statistics and data analysis:

No animals were excluded from analysis. Animals were assigned to experimental groups at random; for experiments comparing a sham mSYMPX to mSYMPX, one animal per cage received each treatment. Behavioral time course data were analyzed using two-way repeated measures ANOVA, with Bonferroni's multiple comparisons posttest to determine on which days experimental groups differed if a significant main effect of experimental group was observed. For these data, the overall F value for the group comparison (e.g. mSYMPX vs. sham mSYMPX, or CCL2-siRNA vs. control siRNA) is given as $F_{(\text{degrees freedom in numerator, degrees freedom in denominator})}$. For experiments involving behavioral measurements the experimenter was blinded to the experimental status starting at the time of surgery. Differences in immunohistochemical staining from sections of DRG or nerve were analyzed with one-way ANOVA with Newman-Keuls Multiple Comparison posttest comparing each group to every other group; ANOVA was used because all histochemical experiments contained 3 groups, namely experimental manipulation, control manipulation, and naïve uninjured rats. For all immunohistochemical experiments, data from 2 – 5 sections in each animal were averaged to obtain a single value for that animal, which was used for the analysis. The statistical test used in each case is indicated in the text, or figure

legend. Two-sided tests were used throughout. Significance was ascribed for $p < 0.05$. Levels of significance are indicated by the number of symbols, e.g., *, $p = 0.01$ to < 0.05 ; **, $p = 0.001$ to 0.01 ; ***, $p < 0.001$. Data are presented as average \pm S.E.M.

RESULTS

mSYMPX reduces mechanical pain behavior induced by tibial nerve crush

After tibial nerve crush, mechanical hypersensitivity was observed with von Frey filaments (testing in the spared sural region of the paw), along with dynamic allodynia (responses to light strokes with a cotton wisp), and cold allodynia (withdrawal responses to acetone stimuli). Guarding behavior, a measure of spontaneous pain⁶⁵ was also increased. In contrast to the prolonged behaviors observed in the original SNI model (cutting and ligation of tibial and common peroneal nerve)^{15,62}, these tibial crush-induced behaviors resolved within 20 – 30 days (Fig. 1). When mSYMPX was performed just prior to the tibial crush, the von Frey and dynamic allodynia responses were significantly reduced throughout the entire time course. However, mSYMPX did not have any effect on cold allodynia. Results were generally similar in males compared to females, except that guarding was overall higher in females and reduced by mSYMPX, while the spike in guarding at day 4 in the sham + crush group was driven by males, as shown in Supplemental Figs. 1 and 2. Contralateral guarding and dynamic mechanical allodynia responses were never observed in either group, and the contralateral von Frey responses remained near baseline. Some acetone responses were observed at baseline and on the contralateral paw, but these were much lower than the responses observed on the ipsilateral side and were not affected by the (ipsilateral) mSYMPX (Supplemental Figs. 1 and 2).

mSYMPX reduces regeneration-associated molecules

We previously showed that the peripheral nerve regeneration process is associated with pain behaviors in the both the spinal nerve ligation model and the SNI model, and that knockdown of GAP43 reduces pain behaviors in the spinal nerve ligation model⁶². More recently, we reported that mSYMPX reduces pain behaviors, regeneration, and GAP43 expression in both of these models⁶³. In the tibial crush model, we also observed the expected upregulation of GAP43 in both the DRG and the distal nerve segment (just distal to the crush site), as observed on day 4 when behavioral responses are near their peak (Fig. 2). This upregulation was reduced by mSYMPX performed at the time of tibial crush. GAP43 is transported by fast axonal transport³⁹; since this can reach speeds of 200 – 400 mm per day⁵² and the nerve injury site is ~70 – 90 mm distal to the DRG cell bodies, some of the observed changes in tibial nerve expression at day 4 could plausibly result from increased expression in DRG neurons. However, the nerve injury site likely has other cellular sources of GAP43, such as Schwann cells^{12,50}; our analysis did not distinguish between axonal and non-axonal GAP43. The reduction in tibial GAP43 after mSYMPX (66%) was greater than could be accounted for just by the loss of sympathetic fibers, which are (by fiber count) ~39% of tibial axons in normal rats⁴⁸.

We also examined the effect of nerve crush on expression of activating transcription factor 3 (ATF3). This transcription factor is upregulated early after axotomy of peripheral axons,

and plays a central role in the process of neurite outgrowth^{8,24,49,56}, though it may not be the transcription factor directly responsible for the increase in GAP43^{20,49}. As shown in Fig. 3, ATF3 -positive neurons were observed in the lumbar DRGs 4 days after nerve crush, and the intensity of the ATF-3 signal was attenuated by mSYMPX.

mSYMPX reduces functional measures of regeneration

The observed reduction in GAP43 and ATF3 suggested that mSYMPX might be acting to reduce regeneration of the tibial axons after tibial nerve crush. To confirm this, in vivo fiber recording was used to measure functional regeneration on day 10 after tibial nerve crush plus mSYMPX or tibial nerve crush plus sham mSYMPX. A stimulating electrode (stimulating at A-fiber strength; hence measuring the degree to which sensory and motor fibers had not only regenerated, but remyelinated) was placed on the tibial nerve distal to the nerve crush site and compound action potentials were measured on the sciatic nerve near its origin where the L4 – L6 spinal nerves converge. Then the stimulating electrode was moved to a point on the tibial nerve proximal to the crush site and the compound action potential measured again (Fig. 4A, B). To estimate the fraction of axons that had failed to completely regenerate and remyelinate through the injury site to the distal, the ratio of the peak of the compound action potential from the distal stimulation to that of the proximal stimulation was analyzed. As shown in Fig. 4C, this ratio was significantly lower in the rats that received mSYMPX. At the end of the fiber recording session, the ipsilateral and contralateral gastrocnemius muscles (that are innervated by the tibial nerve) were removed and weighed. The ratio was analyzed as a measure of denervation-induced atrophy of the muscle; in the short term this atrophy is reversible with reinnervation^{29,66}. As shown in Fig. 4D, the atrophy of the muscle 10 days after tibial crush was greater in rats that received mSYMPX, consistent with a reduction in functional reinnervation. This atrophy is generally taken as a measure of functional motor reinnervation although it can also be somewhat affected by sensory denervation, albeit on a slower time course⁶⁶. A mouse study detected some loss of gastrocnemius muscle weight within a week following tibial nerve transection⁵. The rapid recovery we observed of various functional and behavioral measures including muscle atrophy at day 10 likely reflects the mildness of the crush injury we employed; functional recovery in most nerve crush models that use much longer crush times is generally slower, but improvement of various functional recovery measures between days 7 and 14 in rats has also been shown in some other rat studies using a mild tibial crush similar to that employed here^{36,42}. Peripheral nerve regeneration rates up to 4 mm/day have been reported in rats⁴⁷; for reference, in our study the crush site was ~10 mm from the site of the tibial nerve insertions into the gastrocnemius muscles. Both the CAP measurements and the muscle weight measurements may also depend on the rate of remyelination.

Tibial nerve crush-induced increases in CCL2 and macrophage density are reduced by mSYMPX

The type 1 cytokine CCL2 is increased in the DRG in a variety of pain models^{6,8}, and we showed it was reduced by mSYMPX in a DRG inflammation model⁶⁰. We examined the effect of mSYMPX and nerve crush on CCL2 levels on day 4. As shown in Fig. 5, tibial nerve crush increased levels of CCL2 in DRG neurons as well as in the distal tibial nerve

segment, and these increased levels were reduced by mSYMPX performed at the time of nerve crush although in nerve the effect of mSYMPX did not reach significance.

One primary function of CCL2 is to attract macrophages. As expected from the reduction of CCL2, mSYMPX also mitigated the crush-induced increase in macrophage levels (Iba-1 signal) in the DRG. Iba-1 levels in the distal nerve were increased by the tibial crush but again the effect of mSYMPX did not reach significance (Fig. 6).

The more robust effect of mSYMPX on CCL2 and macrophage density in the DRG compared to the tibial nerve may reflect the fact that there are additional nonneuronal sources of CCL2 at the distal nerve site, such as Schwann cells⁶⁸. However, some of the CCL2 measured in the tibial nerve was likely transported from the DRG; staining in the nerve fibers was evident (Fig. 5B), and like GAP43, CCL2 is likely transported by the fast axonal transport system (since it is processed into large dense core vesicles via the trans-Golgi network²⁷), and hence could plausibly reach the site by day 4 after nerve crush.

CCL2 knockdown reduces pain behaviors

In addition to its roles in various pain models, CCL2 also plays a central role in regeneration⁶⁸. Therefore we were interested in determining whether localized knockdown of CCL2 in the DRG could mimic most aspects of mSYMPX in the tibial crush model. We injected siRNA directed against CCL2, or control nontargeting siRNA, into the L4 and L5 DRGs just prior to tibial nerve crush. As shown in supplemental Fig. 3, the siRNA directed against CCL2 completely mitigated the crush-induced increase of CCL2 in the DRG as measured 4 days later, validating the effectiveness of the siRNA constructs. As shown in Fig. 7 and supplemental Fig. 4, the CCL2 knockdown led to large but incomplete reduction of mechanical hypersensitivity (both static and dynamic), very similar to the effects of mSYMPX. Overall guarding scores appeared somewhat higher and more prolonged in this group of animals (compare to Fig. 1), but, as for mSYMPX, the effect of CCL2 knockdown on guarding was more modest. The main difference between CCL2 knockdown and mSYMPX was that only the former had a marked effect on cold allodynia. Effects on mechanical sensitivity were very similar.

CCL2 knockdown reduces macrophage density

As expected given its role as a key attractant for macrophages, CCL2 knockdown at the time of tibial nerve crush also reduced the Iba-1 signal in the DRG and in the proximal segment of the crushed nerve (Fig. 8).

CCL2 knockdown reduced regeneration-related molecules in the DRG.

Next, we examined the effect of CCL2 knockdown on regeneration-associated molecules in the DRG. As shown in Fig. 9, CCL2 knockdown abrogated the crush-induced increase in GAP43, and partially ameliorated the crush-induced increase in ATF3. In experiments in which ATF3 and the neuronal marker NeuN were co-labeled, the percentage of ATF3-positive neurons was 0 ± 0 (normal DRG), 23.9 ± 3.2 (tibial crush plus non-targeting siRNA), and 7.4 ± 3.1 (tibial crush plus CCL2-targeting siRNA); the nontargeting group was significantly higher than the other two groups (one-way ANOVA with Newman-Keuls

posttest, $F_{(2,9)} = 1.85$, $n = 4$ rats/group). This is consistent with previous studies showing that in the rat L4 DRG ~27% of neurons project in the tibial nerve^{16,54} and with studies showing that ATF3 expression is low in normal DRG neurons and is primarily upregulated in cells with injured axons in peripheral nerve injury models²⁴. However, we cannot rule out the possibility that some of the ATF3- or GAP43-expressing neurons did not project in the tibial nerve, in particular, that in some neurons upregulation may have been related to injury responses to the mSYMPX or sham mSYMPX surgery.

After mSYMPX, no further behavioral effects of CCL2 knock-down are observed

The many similarities between effects of mSYMPX and effects of CCL2 knockdown suggest that the reduction of CCL2 by mSYMPX may account for many of the other observed effects of mSYMPX. If this is the case, then CCL2 knockdown should have little additional effect in animals that have received mSYMPX. This hypothesis was tested by comparing the behavioral effects of CCL2 siRNA vs. nontargeting control siRNA in animals that had all received mSYMPX. Since most behavioral effects of mSYMPX were incomplete, it would have been feasible to detect further improvement in pain behaviors. However, in general additional improvement in behavior measures could not be observed by knocking down CCL2 in animals that had also received mSYMPX (Fig. 10 and supplemental Fig. 5). There was no overall effect of siRNA type in mSYMPX animals on the von Frey threshold, dynamic allodynia test, or guarding scores. Both groups had near maximal cold allodynia scores after tibial crush, similar to those seen with mSYMPX alone. Taken as a whole, the data were consistent with the idea that many mSYMPX effects on mechanical and spontaneous pain can be accounted for by the blockade of tibial crush-induced CCL2 upregulation.

Discussion

CCL2 has been well studied for its roles in both pain¹¹ and peripheral nerve regeneration⁶⁸, but few studies have linked these two roles. Like many other type 1 cytokines, it is upregulated in the DRG in several neuropathic pain models involving peripheral nerve injury³², where in addition to its ability to summon macrophages, it may have direct pro-nociceptive effects due to its direct excitatory effects on sensory neurons (that become more sensitive to CCL2 after injury), and its release from sensory terminals in spinal cord dorsal horn^{10,55,57,58,68}. CCL2 receptor knockout mice lack mechanical allodynia behaviors in a neuropathic pain model¹. CCL2 is identified as a key player in peripheral nerve regeneration, acting at both DRG and peripheral nerve sites⁶⁸. These regeneration studies often use either the sciatic nerve transection model, which does allow pain behavior measurements, or on enhancement of the sensory neuron regeneration response by a prior “conditioning” peripheral injury, due to the induction of regeneration associated genes (“RAGs”) by the conditioning injury. Studies of conditioning usually focus on neurite or axon growth in vitro or in vivo, not pain behaviors. CCL2 has been identified as a RAG, upregulated very early after peripheral but not dorsal root injury of sensory neuron axons. It has been implicated in the conditioning response⁴¹. Kwon et al.³¹ demonstrated that CCL2 plays a role in this response by promoting an M2 phenotype of macrophages in the DRG to promote regeneration. This effect was also observed with intra-DRG injection of CCL2,

but not of 2 other chemokines, CX3CL1 or MIP1 α , though these also increased macrophage density in the DRG as measured by Iba1 staining. Thus, although the latter two type 1 cytokines have also been implicated in neuropathic pain and also have excitatory effects on sensory neurons^{19,35}, CCL2 seems to have a distinct role in promoting regeneration. In mice, CCL2 genetic knock-out reduces the conditioning response⁶⁸ as well as reducing mechanical allodynia behaviors in a neuropathic pain model¹. Knockout of CCR2, the primary receptor for CCL2, also reduces the immune response in DRG after peripheral injury³⁴, while overexpression of CCL2 in the DRG is sufficient to enhance the regenerative capacity of DRG neurons⁴⁰.

The DRG is one likely site of action for both mSYMPX and CCL2 knock-down effects, but peripheral sites of mSYMPX action may contribute, since mSYMPX also reduces sympathetic innervation in the sciatic nerve, local lymph nodes, and paw. Behavioral effects of both procedures were evident at the earliest time point tested (1 day after nerve crush), and at day 4 when the immunohistochemical observations were performed. This makes it unlikely that these effects could be due to reduction of sympathetic sprouting around DRG neurons, as this occurs much more slowly after peripheral nerve injury^{38,43,45,53}. However, we previously found that the mSYMPX procedure rapidly modulated the density of macrophages in the DRG, even in the absence of any injury or inflammatory stimulus⁶³. In a model in which the DRG was directly inflamed, reduction of the inflammation-induced type 1 cytokines in the DRG (including CCL2) by mSYMPX could be observed even one day after DRG inflammation⁶⁰. Although CCL2 has multiple cellular sources and also plays a role in the distal segment in peripheral nerve regeneration models⁶⁸, the siRNA injected within the DRG just prior to the crush would at early time points presumably primarily affect CCL2 expression in DRG neurons. The importance of neuro-immune interactions within the DRG in both pain and regeneration has been highlighted by several studies^{23,27,30,41,68}, including a study showing that surgical lumbar sympathectomy reduced macrophage infiltration in the DRG after sciatic nerve transection³⁷.

Further studies are needed to elucidate the relationship between regeneration, pain, and sympathetic nerves. In the DRG, some possible explanations for our findings are: The marked mSYMPX-induced shift from type 1 towards type 2 cytokines⁶⁰, may reduce both sensory neuron excitability (since many type 1 cytokines including CCL2 are excitatory for sensory neurons) and CCL2 release in the spinal cord, and hence pain behaviors. The mSYMPX-induced reduction of regeneration is harder to explain, since type 2 inflammation generally promotes regeneration and repair; however, regeneration may require an initial period of type 1 inflammation, or these effects may be explained by the special role of CCL2 in regeneration. In addition, not only nerve injury but activation of the innate immune system can increase expression of ATF3²⁴ and Gap43²¹, so perhaps regeneration is less effective when mSYMPX reduces type 1 inflammation. Since behavior effects are observed at early time points, behavioral effects of mSYMPX must rely on effects on intact neurons and/or the reduction of crush-induced excitation in the spinal cord.

We showed that DRG expression of two key regeneration-associated molecules, GAP43 and ATF3, was reduced by mSYMPX and by CCL2 knockdown in the tibial crush model. In various models, altering expression of either of these two molecules can reduce

peripheral regeneration^{17,20–22,24,49}. Concurring with these studies, we observed reduction in several functional regeneration measures by mSYMPX. In combination with our previous studies in other neuropathic pain models, we have consistently shown an association of reduced mechanical hypersensitivity with procedures that reduce peripheral regeneration or regeneration associated molecules (not only mSYMPX but also GAP43 knockdown and application of semaphorin 3A, an inhibitor of axonal outgrowth)^{60,63}. In this study, we chose the tibial crush model as one in which the regeneration process was likely to result in successful reinnervation, as compared to the SNI model in which reinnervation is not possible and the regeneration process results in neuroma formation. Interestingly, in the SNI model we were able to demonstrate that both mSYMPX and semaphorin 3A application were still able to reduce pain behaviors when applied 14 days after the original injury, when pain behaviors were well established^{60,63}. We also found that mSYMPX could still reduce GAP43 expression at this time point, agreeing with original studies suggesting its expression is maintained until target reinnervation can occur⁵⁹. In the present study, the duration of mechanical hypersensitivity was short enough that repeating the experiment of performing mSYMPX on day 14 was not very practical.

A limitation of the study is use of immunohistochemistry methods to quantify expression of CCL2, GAP43, and ATF3; while we took care to minimize confounds by keeping immunostaining conditions and image acquisition parameters constant, other confounds such as condition-based epitope masking may be present. The immunohistochemistry method was selected for the study because we wished to view and analyze the cellular localization of the molecules; their upregulation in DRG neurons and/or axons after peripheral nerve injury was already well established, but we did not know what effect local sympathectomy might have on the cell types expressing these molecules. Although we detected reduced intensity of GAP43 and ATF3 with immunohistochemistry, we cannot be certain these changes had meaningful effects on regeneration. In addition, the immunohistochemistry method used may not be sensitive enough to detect all neurons expressing GAP43, as some studies show higher basal expression than we observed.

In this study, mSYMPX markedly reduced mechanical hypersensitivity, but the effect was only partial. We also observed partial behavioral effects of mSYMPX in other neuropathic pain models (SNI, spinal nerve ligation), and a DRG compression model of low back pain. In these various models the von Frey threshold was restored from very low values (<1 gram) in sham or naive rats to 7 – 9 grams in mSYMPX animals (as measured on day 3 or 4 after implementing the model), compared to baseline values in uninjured animals having values near the cutoff of 15 grams (see ^{63,64} and Fig. 1). The largest observed effects of mSYMPX were in the model in which the DRG is directly inflamed by local application of the immune activator zymosan (12 gram von Frey threshold in mSYMPX animals) and the model in which the paw is inflamed with complete Freund's adjuvant (11 grams)⁶⁰. These results are also consistent with the idea that the primary effect of mSYMPX is on local immune processes; the neuropathic models perhaps include both an immune component and additional components related to non-immune aspects of the axotomy or axonal damage cell body response. More specifically, our results are also consistent with the idea that blockade of CCL2 increases can account for many observed effects of mSYMPX. In a comprehensive bioinformatics study of gene expression changes involved with sensory

neuron regeneration, incorporating data from multiple nerve injury models, it was noted that overexpression of a single RAG alone, even those transcription factors that represented core “hubs” of the regeneration network such as ATF3, was not sufficient to completely effect successful regeneration⁸. Several studies suggest that the molecules we found to be regulated by mSYMPX in the nerve crush model (CCL2, GAP43, and ATF3) are not always regulated concordantly^{13,20,49,68}. Insofar as the regeneration process and pain behaviors are linked, a further understanding of the network properties may be essential to understanding whether it is possible to block development of neuropathic pain without blocking peripheral nerve regeneration, in conditions in which such regeneration is possible and desirable.

Supplementary Material

Refer to Web version on PubMed Central for supplementary material.

Acknowledgements:

Supported by NIH grants National Institute of Neurological Disorders and Stroke (NS045594 to J-MZ), National Institute of Arthritis and Musculoskeletal and Skin Diseases (AR068989 to J-MZ), Bethesda, MD, USA. X.Z. was supported in part by a grant from the National Natural Science Fund of China (No. 81400916). The authors declare no conflicts of interest. The authors thank Debora De Nardin Lückemeyer for conducting the Elisa study and Sarah Pixley for helpful discussions.

References

- [1]. Abbadie C, Lindia JA, Cumiskey AM, Peterson LB, Mudgett JS, Bayne EK, DeMartino JA, MacIntyre DE, Forrest MJ. Impaired neuropathic pain responses in mice lacking the chemokine receptor CCR2. *Proc Natl Acad Sci U S A* 2003;100(13):7947–7952. [PubMed: 12808141]
- [2]. Allen JE, Sutherland TE. Host protective roles of type 2 immunity: parasite killing and tissue repair, flip sides of the same coin. *Semin Immunol* 2014;26(4):329–340. [PubMed: 25028340]
- [3]. Bajrovic F, Sketelj J. Extent of nociceptive dermatomes in adult rats is not primarily maintained by axonal competition. *Exp Neurol* 1998;150(1):115–121. [PubMed: 9514823]
- [4]. Baron R, Jänig W, Kollmann W. Sympathetic and afferent somata projecting in hindlimb nerves and the anatomical organization of the lumbar sympathetic nervous system of the rat. *J Comp Neurol* 1988;275(3):460–468. [PubMed: 3225349]
- [5]. Batt JA, Bain JR. Tibial nerve transection - a standardized model for denervation-induced skeletal muscle atrophy in mice. *J Vis Exp* 2013(81):e50657. [PubMed: 24300114]
- [6]. Biber K, Boddeke E. Neuronal CC chemokines: the distinct roles of CCL21 and CCL2 in neuropathic pain. *Front Cell Neurosci* 2014;8:210. [PubMed: 25147499]
- [7]. Bönhof GJ, Strom A, Püttgen S, Ringel B, Brüggemann J, Bódis K, Müssig K, Szendroedi J, Roden M, Ziegler D. Patterns of cutaneous nerve fibre loss and regeneration in type 2 diabetes with painful and painless polyneuropathy. *Diabetologia* 2017;60(12):2495–2503. [PubMed: 28914336]
- [8]. Chandran V, Coppola G, Nawabi H, Omura T, Versano R, Huebner EA, Zhang A, Costigan M, Yekkiral A, Barrett L, Blesch A, Michaelevski I, Davis-Turak J, Gao F, Langfelder P, Horvath S, He Z, Benowitz L, Fainzilber M, Tuszynski M, Woolf CJ, Geschwind DH. A Systems-Level Analysis of the Peripheral Nerve Intrinsic Axonal Growth Program. *Neuron* 2016;89(5):956–970. [PubMed: 26898779]
- [9]. Chaplan SR, Bach FW, Pogrel JW, Chung JM, Yaksh TL. Quantitative assessment of tactile allodynia in the rat paw. *Journal of Neuroscience Methods* 1994;53(1):55–63. [PubMed: 7990513]
- [10]. Chen O, Donnelly CR, Ji RR. Regulation of pain by neuro-immune interactions between macrophages and nociceptor sensory neurons. *Curr Opin Neurobiol* 2019;62:17–25. [PubMed: 31809997]

- [11]. Clark AK, Old EA, Malcangio M. Neuropathic pain and cytokines: current perspectives. *J Pain Res* 2013;6:803–814. [PubMed: 24294006]
- [12]. Curtis R, Stewart HJ, Hall SM, Wilkin GP, Mirsky R, Jessen KR. GAP-43 is expressed by nonmyelin-forming Schwann cells of the peripheral nervous system. *J Cell Biol* 1992;116(6):1455–1464. [PubMed: 1531832]
- [13]. Dauvergne C, Molet J, Reaux-Le Goazigo A, Mauborgne A, Melik-Parsadaniantz S, Boucher Y, Pohl M. Implication of the chemokine CCL2 in trigeminal nociception and traumatic neuropathic orofacial pain. *Eur J Pain* 2014;18(3):360–375. [PubMed: 23918315]
- [14]. Davies AJ, Kim HW, Gonzalez-Cano R, Choi J, Back SK, Roh SE, Johnson E, Gabriac M, Kim MS, Lee J, Lee JE, Kim YS, Bae YC, Kim SJ, Lee KM, Na HS, Riva P, Latremoliere A, Rinaldi S, Ugolini S, Costigan M, Oh SB. Natural Killer Cells Degenerate Intact Sensory Afferents following Nerve Injury. *Cell* 2019;176(4):716–728 e718. [PubMed: 30712871]
- [15]. Decosterd I, Woolf CJ. Spared nerve injury: an animal model of persistent peripheral neuropathic pain. *Pain* 2000;87(2):149–158. [PubMed: 10924808]
- [16]. Devor M, Govrin-Lippmann R, Frank I, Raber P. Proliferation of primary sensory neurons in adult rat dorsal root ganglion and the kinetics of retrograde cell loss after sciatic nerve section. *Somatosens Res* 1985;3(2):139–167. [PubMed: 3835669]
- [17]. Dubovy P, Klusakova I, Hradilova-Svizenska I, Joukal M. Expression of Regeneration-Associated Proteins in Primary Sensory Neurons and Regenerating Axons After Nerve Injury-An Overview. *Anat Rec (Hoboken)* 2018;301(10):1618–1627. [PubMed: 29740961]
- [18]. Elenkov IJ, Wilder RL, Chrousos GP, Vizi ES. The sympathetic nerve--an integrative interface between two supersystems: the brain and the immune system. *Pharmacol Rev* 2000;52(4):595–638. [PubMed: 11121511]
- [19]. Freitag CM, Miller RJ. Peroxisome proliferator-activated receptor agonists modulate neuropathic pain: a link to chemokines? *Front Cell Neurosci* 2014;8:238. [PubMed: 25191225]
- [20]. Gey M, Wanner R, Schilling C, Pedro MT, Sinske D, Knoll B. Atf3 mutant mice show reduced axon regeneration and impaired regeneration-associated gene induction after peripheral nerve injury. *Open Biol* 2016;6(8).
- [21]. Holahan MR. A Shift from a Pivotal to Supporting Role for the Growth-Associated Protein (GAP-43) in the Coordination of Axonal Structural and Functional Plasticity. *Front Cell Neurosci* 2017;11:266. [PubMed: 28912688]
- [22]. Holland SD, Ramer LM, McMahon SB, Denk F, Ramer MS. An ATF3-CreERT2 Knock-In Mouse for Axotomy-Induced Genetic Editing: Proof of Principle. *eNeuro* 2019;6(2).
- [23]. Hu P, McLachlan EM. Distinct functional types of macrophage in dorsal root ganglia and spinal nerves proximal to sciatic and spinal nerve transections in the rat. *Exp Neurol* 2003;184(2):590–605. [PubMed: 14769352]
- [24]. Hunt D, Raivich G, Anderson PN. Activating transcription factor 3 and the nervous system. *Front Mol Neurosci* 2012;5:7. [PubMed: 22347845]
- [25]. Imai Y, Ibata I, Ito D, Ohsawa K, Kohsaka S. A novel gene *iba1* in the major histocompatibility complex class III region encoding an EF hand protein expressed in a monocytic lineage. *Biochem Biophys Res Commun* 1996;224(3):855–862. [PubMed: 8713135]
- [26]. Imai Y, Kohsaka S. Intracellular signaling in M-CSF-induced microglia activation: role of *Iba1*. *Glia* 2002;40(2):164–174. [PubMed: 12379904]
- [27]. Jung H, Toth PT, White FA, Miller RJ. Monocyte chemoattractant protein-1 functions as a neuromodulator in dorsal root ganglia neurons. *J Neurochem* 2008;104(1):254–263. [PubMed: 17944871]
- [28]. Kanazawa H, Ohsawa K, Sasaki Y, Kohsaka S, Imai Y. Macrophage/microglia-specific protein *Iba1* enhances membrane ruffling and Rac activation via phospholipase C-gamma -dependent pathway. *J Biol Chem* 2002;277(22):20026–20032. [PubMed: 11916959]
- [29]. Kobayashi J, Mackinnon SE, Watanabe O, Ball DJ, Gu XM, Hunter DA, Kuzon WM Jr. The effect of duration of muscle denervation on functional recovery in the rat model. *Muscle Nerve* 1997;20(7):858–866. [PubMed: 9179158]

- [30]. Kwon MJ, Kim J, Shin H, Jeong SR, Kang YM, Choi JY, Hwang DH, Kim BG. Contribution of macrophages to enhanced regenerative capacity of dorsal root ganglia sensory neurons by conditioning injury. *J Neurosci* 2013;33(38):15095–15108. [PubMed: 24048840]
- [31]. Kwon MJ, Shin HY, Cui Y, Kim H, Thi AH, Choi JY, Kim EY, Hwang DH, Kim BG. CCL2 Mediates Neuron-Macrophage Interactions to Drive Proregenerative Macrophage Activation Following Preconditioning Injury. *J Neurosci* 2015;35(48):15934–15947. [PubMed: 26631474]
- [32]. LaCroix-Fralish ML, Austin JS, Zheng FY, Levitin DJ, Mogil JS. Patterns of pain: meta-analysis of microarray studies of pain. *Pain* 2011;152(8):1888–1898. [PubMed: 21561713]
- [33]. Levy D, Kubes P, Zochodne DW. Delayed peripheral nerve degeneration, regeneration, and pain in mice lacking inducible nitric oxide synthase. *J Neuropathol Exp Neurol* 2001;60(5):411–421. [PubMed: 11379816]
- [34]. Lindborg JA, Niemi JP, Howarth MA, Liu KW, Moore CZ, Mahajan D, Zigmond RE. Molecular and cellular identification of the immune response in peripheral ganglia following nerve injury. *J Neuroinflammation* 2018;15(1):192. [PubMed: 29945607]
- [35]. Liou JT, Lee CM, Day YJ. The immune aspect in neuropathic pain: role of chemokines. *Acta Anaesthesiol Taiwan* 2013;51(3):127–132. [PubMed: 24148742]
- [36]. Malushte TS, Kerns JM, Huang CC, Shott S, Safanda J, Gonzalez M. Assessment of recovery following a novel partial nerve lesion in a rat model. *Muscle Nerve* 2004;30(5):609–617. [PubMed: 15389719]
- [37]. McLachlan EM, Hu P. Inflammation in dorsal root ganglia after peripheral nerve injury: effects of the sympathetic innervation. *Auton Neurosci* 2014;182:108–117. [PubMed: 24418114]
- [38]. McLachlan EM, Jang W, Devor M, Michaelis M. Peripheral nerve injury triggers noradrenergic sprouting within dorsal root ganglia. *Nature* 1993;363(6429):543–546. [PubMed: 8505981]
- [39]. Nakata T, Terada S, Hirokawa N. Visualization of the dynamics of synaptic vesicle and plasma membrane proteins in living axons. *J Cell Biol* 1998;140(3):659–674. [PubMed: 9456325]
- [40]. Niemi JP, DeFrancesco-Lisowitz A, Cregg JM, Howarth M, Zigmond RE. Overexpression of the monocyte chemokine CCL2 in dorsal root ganglion neurons causes a conditioning-like increase in neurite outgrowth and does so via a STAT3 dependent mechanism. *Exp Neurol* 2016;275 Pt 1:25–37. [PubMed: 26431741]
- [41]. Niemi JP, DeFrancesco-Lisowitz A, Roldan-Hernandez L, Lindborg JA, Mandell D, Zigmond RE. A critical role for macrophages near axotomized neuronal cell bodies in stimulating nerve regeneration. *J Neurosci* 2013;33(41):16236–16248. [PubMed: 24107955]
- [42]. Omura T, Sano M, Omura K, Hasegawa T, Doi M, Sawada T, Nagano A. Different expressions of BDNF, NT3, and NT4 in muscle and nerve after various types of peripheral nerve injuries. *J Peripher Nerv Syst* 2005;10(3):293–300. [PubMed: 16221288]
- [43]. Pertin M, Allchorne AJ, Beggah AT, Woolf CJ, Decosterd I. Delayed sympathetic dependence in the spared nerve injury (SNI) model of neuropathic pain. *Mol Pain* 2007;3:21. [PubMed: 17672895]
- [44]. Pongratz G, Straub RH. The sympathetic nervous response in inflammation. *Arthritis Res Ther* 2014;16(6):504. [PubMed: 25789375]
- [45]. Ramer MS, Bisby MA. Rapid sprouting of sympathetic axons in dorsal root ganglia of rats with a chronic constriction injury. *Pain* 1997;70(2–3):237–244. [PubMed: 9150299]
- [46]. Rickard AJ, Young MJ. Corticosteroid receptors, macrophages and cardiovascular disease. *J Mol Endocrinol* 2009;42(6):449–459. [PubMed: 19158233]
- [47]. Savastano LE, Laurito SR, Fitt MR, Rasmussen JA, Gonzalez Polo V, Patterson SI. Sciatic nerve injury: a simple and subtle model for investigating many aspects of nervous system damage and recovery. *J Neurosci Methods* 2014;227:166–180. [PubMed: 24487015]
- [48]. Schmalbruch H. Fiber composition of the rat sciatic nerve. *Anat Rec* 1986;215(1):71–81. [PubMed: 3706794]
- [49]. Seiffers R, Mills CD, Woolf CJ. ATF3 increases the intrinsic growth state of DRG neurons to enhance peripheral nerve regeneration. *J Neurosci* 2007;27(30):7911–7920. [PubMed: 17652582]
- [50]. Sensenbrenner M, Lucas M, Deloulme JC. Expression of two neuronal markers, growth-associated protein 43 and neuron-specific enolase, in rat glial cells. *J Mol Med (Berl)* 1997;75(9):653–663. [PubMed: 9351704]

- [51]. Sommer C, Schafers M. Painful mononeuropathy in C57BL/Wld mice with delayed wallerian degeneration: differential effects of cytokine production and nerve regeneration on thermal and mechanical hypersensitivity. *Brain Res* 1998;784(1–2):154–162. [PubMed: 9518588]
- [52]. Stenoien DL, Brady ST. Fast Axonal Transport. In: Siegel GJ, Agranoff BW, Albers RW, Fisher SK, Uhler MD, editors. *Basic Neurochemistry: Molecular, Cellular and Medical Aspects* Philadelphia: Lippincott-Raven, 1999.
- [53]. Strong JA, Zhang J-M, Schaible H-G. The Sympathetic Nervous System and Pain. In: Wood JN, editor. *The Oxford Handbook of the Neurobiology of Pain*: Oxford University Press, 2018.
- [54]. Swett JE, Torigoe Y, Elie VR, Bourassa CM, Miller PG. Sensory neurons of the rat sciatic nerve. *Exp Neurol* 1991;114(1):82–103. [PubMed: 1915738]
- [55]. Thacker MA, Clark AK, Bishop T, Grist J, Yip PK, Moon LD, Thompson SW, Marchand F, McMahon SB. CCL2 is a key mediator of microglia activation in neuropathic pain states. *Eur J Pain* 2009;13(3):263–272. [PubMed: 18554968]
- [56]. Tsujino H, Kondo E, Fukuoka T, Dai Y, Tokunaga A, Miki K, Yonenobu K, Ochi T, Noguchi K. Activating transcription factor 3 (ATF3) induction by axotomy in sensory and motoneurons: A novel neuronal marker of nerve injury. *Mol Cell Neurosci* 2000;15(2):170–182. [PubMed: 10673325]
- [57]. Van Steenwinckel J, Reaux-Le Goazigo A, Pommier B, Mauborgne A, Dansereau MA, Kitabgi P, Sarret P, Pohl M, Melik Parsadaniantz S. CCL2 released from neuronal synaptic vesicles in the spinal cord is a major mediator of local inflammation and pain after peripheral nerve injury. *J Neurosci* 2011;31(15):5865–5875. [PubMed: 21490228]
- [58]. White FA, Sun J, Waters SM, Ma C, Ren D, Ripsch M, Steflik J, Cortright DN, Lamotte RH, Miller RJ. Excitatory monocyte chemoattractant protein-1 signaling is up-regulated in sensory neurons after chronic compression of the dorsal root ganglion. *Proc Natl Acad Sci U S A* 2005;102(39):14092–14097. [PubMed: 16174730]
- [59]. Woolf CJ, Reynolds ML, Molander C, O'Brien C, Lindsay RM, Benowitz LI. The growth-associated protein GAP-43 appears in dorsal root ganglion cells and in the dorsal horn of the rat spinal cord following peripheral nerve injury. *Neuroscience* 1990;34(2):465–478. [PubMed: 2139720]
- [60]. Xie W, Chen S, Strong JA, Li A-L, Lewkowich IP, Zhang J-M. Localized sympathectomy reduces mechanical hypersensitivity by restoring normal immune homeostasis in rat models of inflammatory pain. *J Neurosci* 2016;36(33):8712–8725. [PubMed: 27535916]
- [61]. Xie W, Strong JA, Kays J, Nicol GD, Zhang JM. Knockdown of the sphingosine-1-phosphate receptor S1PR1 reduces pain behaviors induced by local inflammation of the rat sensory ganglion. *Neurosci Lett* 2012;515(1):61–65. [PubMed: 22445889]
- [62]. Xie W, Strong JA, Zhang JM. Active Nerve Regeneration with Failed Target Reinnervation Drives Persistent Neuropathic Pain. *eNeuro* 2017;4(1).
- [63]. Xie W, Strong JA, Zhang JM. Localized sympathectomy reduces peripheral nerve regeneration and pain behaviors in 2 rat neuropathic pain models. *Pain* 2020;161(8):1925–1936. [PubMed: 32701850]
- [64]. Xie W, Zhang J, Strong JA, Zhang J-M. Role of NaV1.6 and NaVβ4 sodium channel subunits in a rat model of low back pain induced by compression of the dorsal root ganglia. *Neuroscience* 2019;in press.
- [65]. Xu J, Brennan TJ. Guarding pain and spontaneous activity of nociceptors after skin versus skin plus deep tissue incision. *Anesthesiology* 2010;112(1):153–164. [PubMed: 19996955]
- [66]. Zhao L, Lv G, Jiang S, Yan Z, Sun J, Wang L, Jiang D. Morphological differences in skeletal muscle atrophy of rats with motor nerve and/or sensory nerve injury. *Neural Regen Res* 2012;7(32):2507–2515. [PubMed: 25337102]
- [67]. Zhu A, Shen L, Xu L, Chen W, Huang Y. Wnt5a mediates chronic post-thoracotomy pain by regulating non-canonical pathways, nerve regeneration, and inflammation in rats. *Cell Signal* 2018;44:51–61. [PubMed: 29339085]
- [68]. Zigmond RE, Echevarria FD. Macrophage biology in the peripheral nervous system after injury. *Prog Neurobiol* 2019;173:102–121. [PubMed: 30579784]

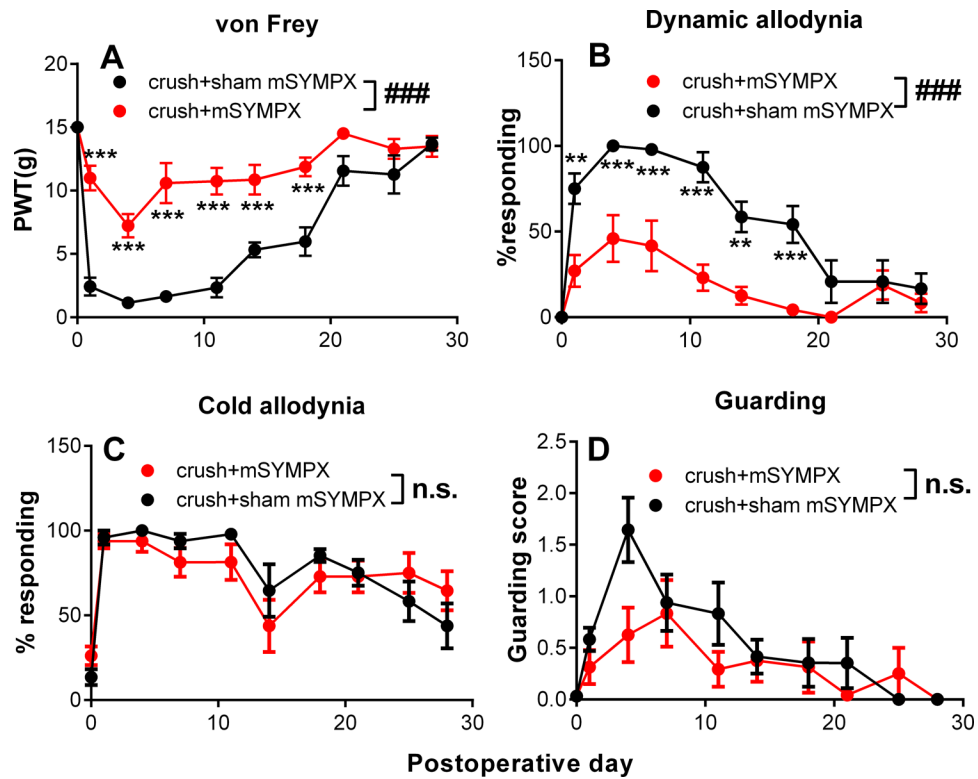


Fig. 1: Effect of micros ympathectomy (“mSYMPX”) on pain behaviors after tibial nerve crush. Baseline behaviors were measured twice prior to surgery, and the average value is plotted on day 0. On day 0, in one surgery, the tibial nerve was exposed and crushed, and the sympathetic grey rami entering L4 and L5 spinal nerves were exposed (sham mSYMPX) or exposed and cut (mSYMPX). ###, $p < 0.001$; significant overall effect of mSYMPX factor (2 way repeated measures ANOVA); $F_{(1,14)} = 54.4$ (A); 25.9 (B); 0.104, $p = 0.75$, not significant (n.s.) (C); and 2.1, $p = 0.17$, not significant (D). In panel A and B the interaction effect was also significant. **, $p < 0.01$; ***, $p < 0.001$; significant difference between the groups at the indicated time point (Bonferroni’s multiple comparisons posttest). $N = 8$ rats/group, 4 of each sex. Data for individual sexes including contralateral data can be observed in Supplemental Figs. 1 and 2.

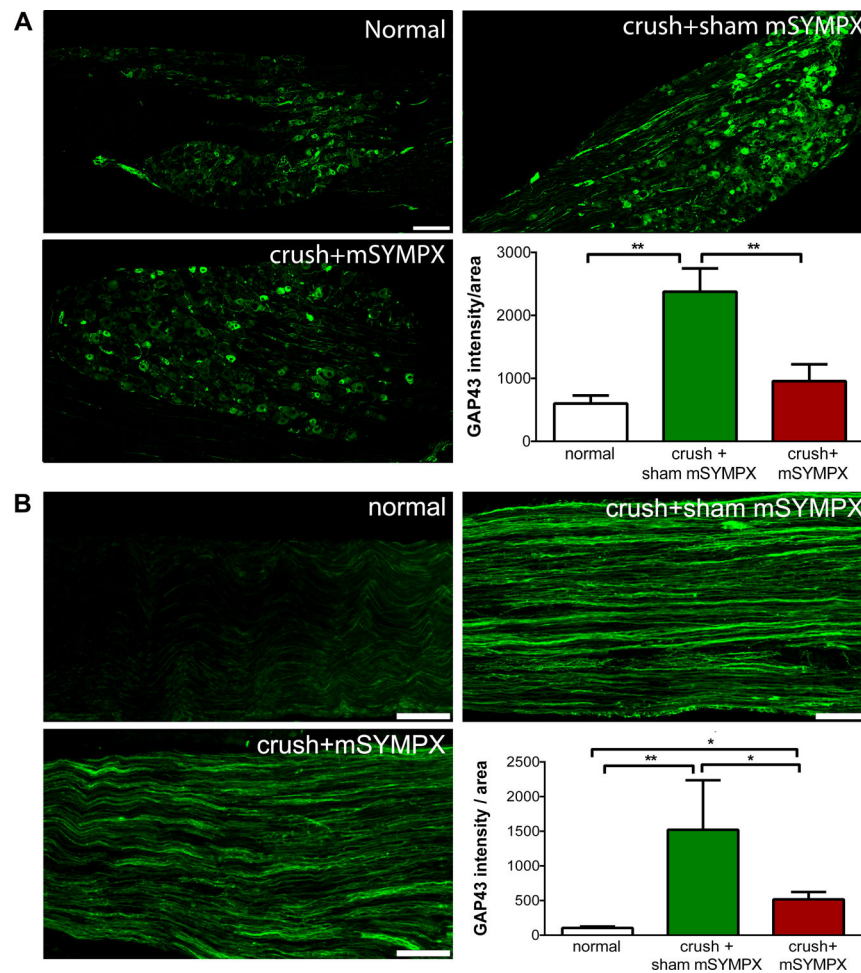


Fig. 2: Effect of mSYMPX on growth-associated protein 43 (GAP43) expression in dorsal root ganglion (DRG) and distal nerve after tibial nerve crush. Four days after tibial nerve crush and mSYMPX or sham mSYMPX, sections of the L4/L5 DRG (A) and longitudinal sections of tibial nerve distal to the nerve crush site (B) were obtained and examined with immunostaining for GAP43. Normal DRG and tibial nerve from unoperated rats were also examined. Example sections are shown for each of the three groups. Scale bar = 200 μ m. Summary data: *, $p < 0.05$; **, $p < 0.01$; significant difference between indicated groups, one-way ANOVA with Newman-Keuls Multiple Comparison posttest, $F_{(2,9)} = 11.78$ (A), 3.049 (B). $N = 4$ rats per group (both sexes).

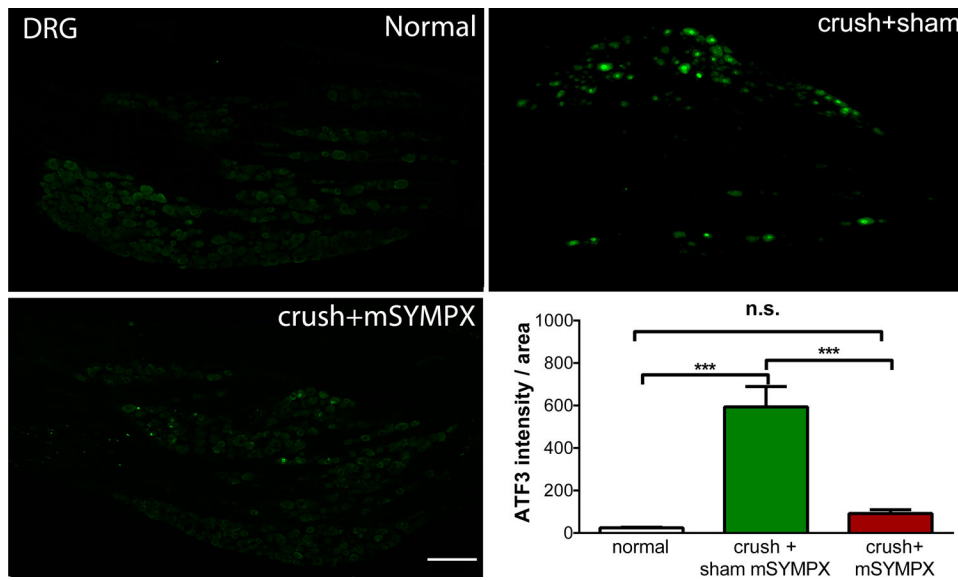


Fig. 3: Effect of mSYMPX on activating transcription factor 3 (ATF3) expression in dorsal root ganglion (DRG) after tibial nerve crush. Four days after tibial nerve crush and mSYMPX or sham mSYMPX, sections of the L4/L5 DRG were obtained and examined with immunostaining for ATF3. Normal DRG were also examined. ***, $p < 0.001$; significant difference between the indicated groups, one-way ANOVA with Newman-Keuls Multiple Comparison posttest, $F_{(2,9)} = 30.95$. $N = 4$ animals per group (both sexes). n.s., not significant.

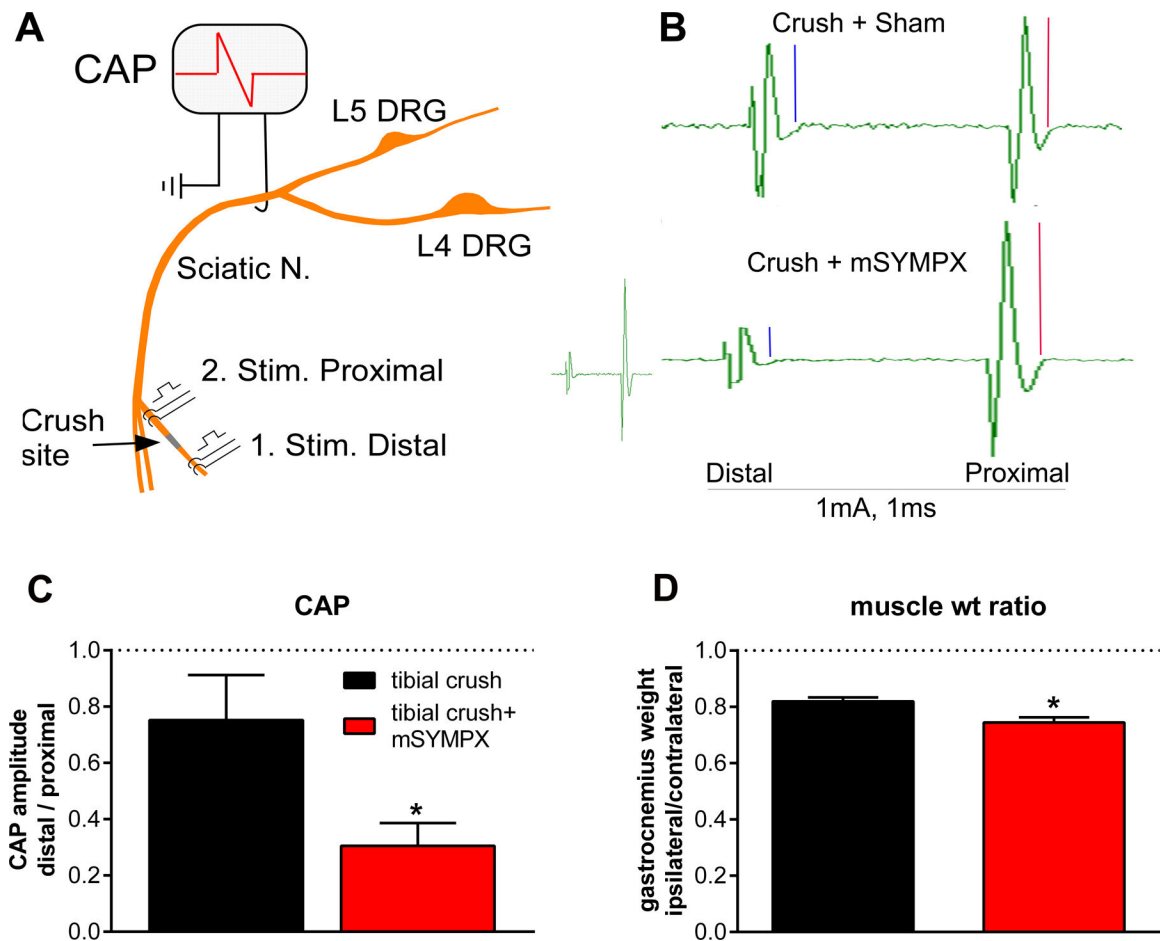


Fig. 4. Effect of mSYMPX on functional measures of nerve regeneration. Ten days after tibial crush injury, with or without concomitant mSYMPX, compound action potentials (CAP) were measured in response to stimulation distal to the crush site, then proximal to the crush site. **A.** In vivo recording setup. The recording electrode was on the sciatic nerve just after its formation from the merging L4, L5, and L6 (not shown) spinal nerves. The stimulating electrode was placed on the tibial nerve, just distal to the crush, and CAP evoked. Then the stimulating electrode was moved proximal to the crush site. Stimuli were 1 msec, 1mA pulses (A-fiber strength). **B.** Examples of CAP evoked with distal (left) and proximal (right) stimuli. The early peaks (corresponding to the number of A- α and A- β fibers) were measured (blue, distal peak; red, proximal peak) and their ratio is plotted in **C**; a value of 1 would be expected in a normal nerve, and a value of 0 would indicate no fibers had regenerated through the injury site. **D.** The lateral and medial gastrocnemius muscle (innervated by the crushed tibial nerve) and its contralateral counterpart were dissected out on day 10, immediately after the CAP recording, and weighed. The ratio of the ipsilateral to contralateral weight is plotted; a value of 1 is expected in normal animals and smaller numbers indicate greater denervation-induced muscle atrophy. N = 5 rats per group. *, $p < 0.05$, significantly different from tibial crush group, t-test.

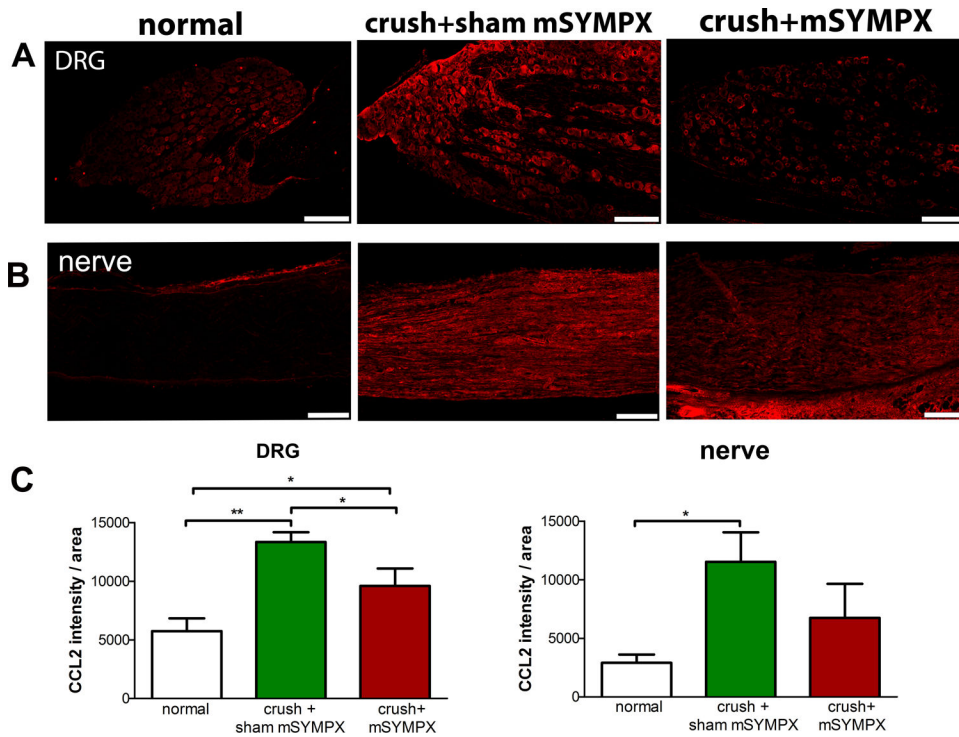


Fig. 5: Effect of mSYMPX on expression of CCL2 expression in dorsal root ganglion (DRG) and distal nerve after tibial nerve crush. Four days after tibial nerve crush and mSYMPX or sham mSYMPX, sections of the L4 DRG (A) and tibial nerve distal to the nerve crush site (B) were obtained and examined with immunostaining for CCL2 (red). Normal DRG and tibial nerve from unoperated rats were also examined. Example sections are shown for each of the three groups. Scale bar=200 μ m. Summary data (C): *, $p<0.05$; **, $p<0.01$; significant difference between indicated groups, one-way ANOVA with Newman-Keuls Multiple Comparison posttest. $F_{(2,9)}= 3.55$ (A), 4.46 (B). $N = 3-4$ animals per group (both sexes).

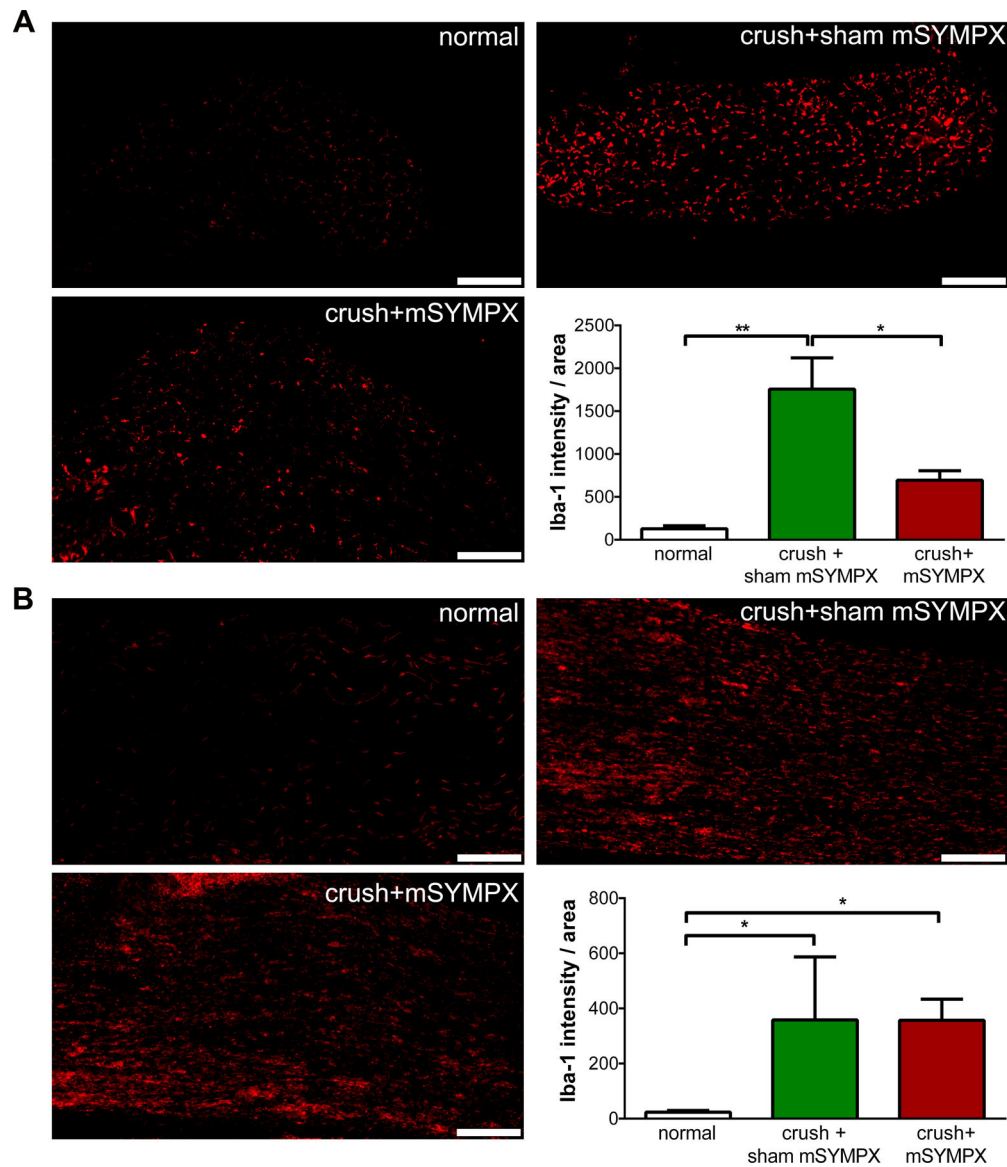


Fig. 6: Effect of mSYMPX on expression of pan macrophage marker ionized calcium-binding adapter molecule 1 (Iba-1) in dorsal root ganglion (DRG) and distal nerve after tibial nerve crush. Four days after tibial nerve crush and mSYMPX or sham mSYMPX, sections of the L4 DRG (A) and tibial nerve distal to the nerve crush site (B) were obtained and examined with immunostaining for Iba-1 (red). Normal DRG and tibial nerve from unoperated rats were also examined. Same animals and DRG sections as Fig. 2. Example sections are shown for each of the three groups. Scale bar = 200 μ m. Summary data graphs: *, $p < 0.05$; **, $p < 0.01$; significant difference between indicated groups, one-way ANOVA with Newman-Keuls Multiple Comparison posttest, $F_{(2,8)} = 10.03$ (A), 2.95 (B). $N = 4$ animals per group.

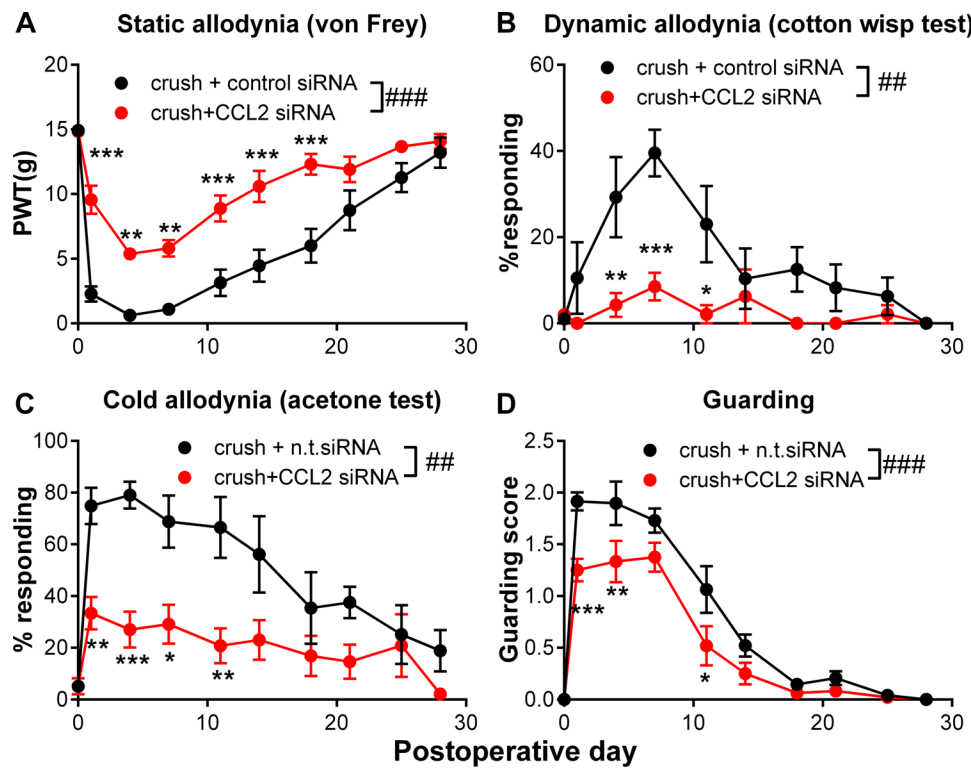


Fig. 7. Effect of CCL2 knockdown on pain behaviors after tibial nerve crush. Baseline behaviors were measured twice prior to surgery, and the average value plotted on day 0. On day 0, in one surgery, the tibial nerve was exposed and crushed, and siRNA directed against CCL2 or nontargeting control was injected into the L4 and L5 DRGs. A, Paw withdrawal threshold (PWT), von Frey test. B, Dynamic allodynia (cotton wisp test). C, Cold allodynia (acetone test). D, Guarding score (maximum score = 3). ##, $p < 0.01$; ###, $p < 0.001$; significant overall effect of the siRNA type (2 way repeated measures ANOVA); $F_{(1,14)} = 36.9$ (A), 9.55 (B), 11.7 (C), and 28.5 (D). In each panel the interaction effect was also significant. *, $p < 0.05$; **, $p < 0.01$; ***, $p < 0.001$; significant difference between the groups at the indicated time point (Bonferroni's multiple comparisons posttest). Data for individual sexes can be found in Supplemental Fig. 4.

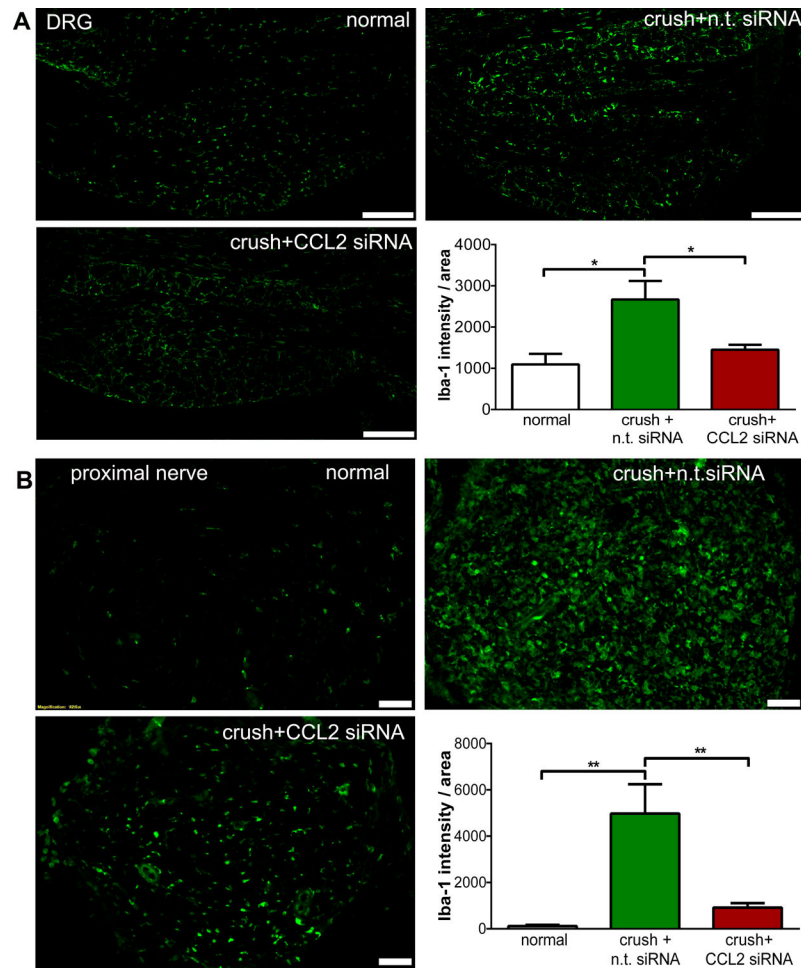


Fig. 8: Effect of CCL2 knockdown on expression of pan macrophage marker ionized calcium-binding adapter molecule 1 (Iba-1) in the DRG and proximal nerve. In one surgery, the tibial nerve was exposed and crushed, and siRNA directed against CCL2 or nontargeting (n.t.) control was injected into the L4 and L5 DRGs. Four days later, L4/L5 DRG sections (A) and nerve sections proximal to the nerve crush (B) were obtained and stained for Iba1. Normal L4/L5 DRG and nerve sections from uninjured rats were also collected. Example sections from each of the 3 experimental groups are shown. Summary data: *, $p < 0.05$; **, $p < 0.01$; significant difference between the indicated groups, one-way ANOVA with Newman-Keuls Multiple Comparison posttest, $F_{(2,9)} = 6.65$ (A); 12.27 (B). $N = 3 - 4$ rats/group (A) and a different set of 4 rats/group (B).

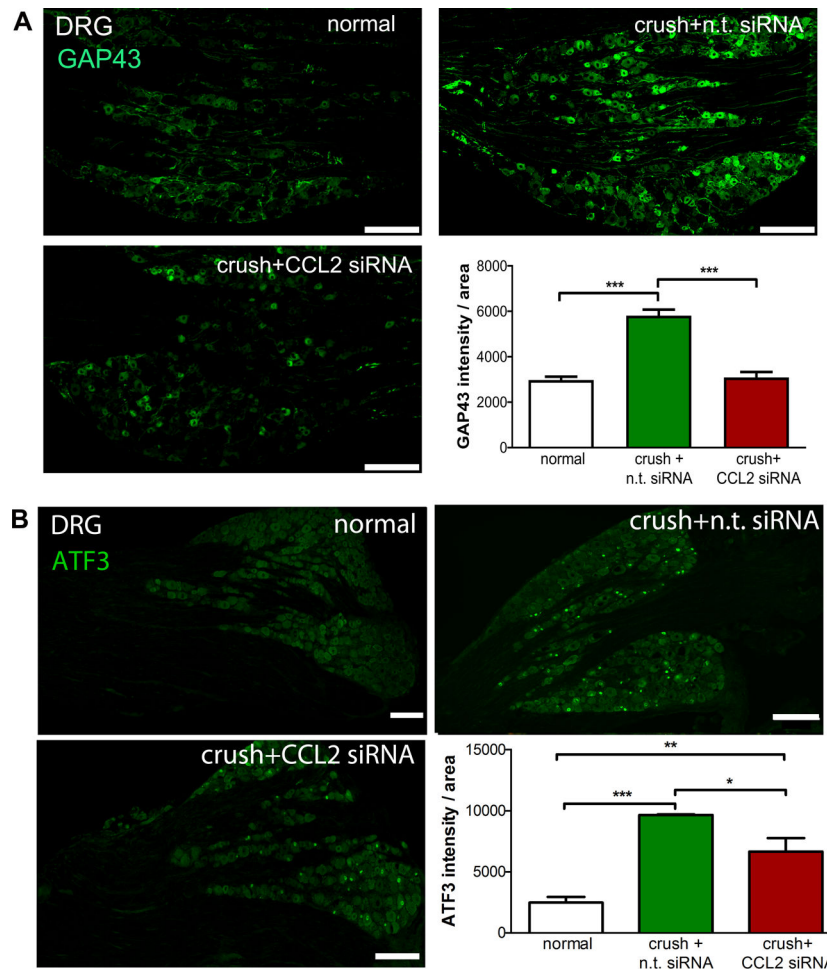
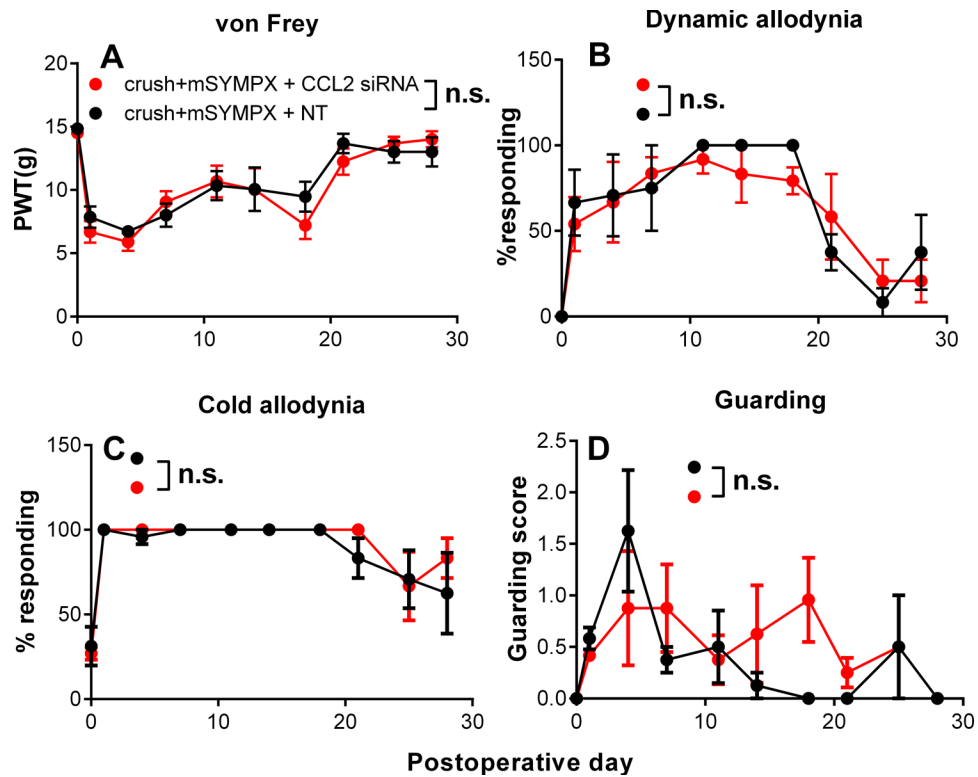


Fig. 9: Effect of CCL2 knockdown on regeneration associated molecules in the DRG. In one surgery, the tibial nerve was exposed and crushed, and siRNA directed against CCL2 or nontargeting control was injected into the L4 and L5 DRGs. Four days later, L4/L5 DRG sections were stained for (A) growth associated protein 43 (GAP43) or (B) activating transcription factor 3 (ATF3) 4 days later. Normal L4/L5 DRG from uninjured rats were also collected. Example sections from each of the 3 experimental groups are shown. Summary data: ***, $p < 0.001$; **, $p < 0.01$; *, $p < 0.05$; significant difference between the indicated groups, one-way ANOVA with Newman-Keuls Multiple Comparison posttest, $F_{(2,8)} = 46.3$ (A); $F_{(2,9)} = 27.45$ (B). $N = 3-4$ rats/group (A) and a different set of 4 rats/group (B).

**Fig. 10.**

Effect of CCL2 knockdown on pain behaviors after tibial nerve crush plus mSYMPX.

Baseline behaviors were measured twice prior to surgery, and the average value plotted on day 0. On day 0, in one surgery, the tibial nerve was exposed and crushed, mSYMPX was performed, and siRNA directed against CCL2 or nontargeting control was injected into the L4 and L5 DRGs. A, Paw withdrawal threshold (PWT), von Frey test. B, Dynamic allodynia (cotton wisp test). C, Cold allodynia (acetone test). D, Guarding score (maximum score = 3). n.s., not significant; no overall effect of the siRNA type (2 way repeated measures ANOVA); $F_{(1,14)} = 8.9$, $p = 0.20$, n.s. (A), 1.8, $p = 0.2$, n.s. (B), 4.7 (C), and 1.25, $p = 0.28$, n.s. (D). In each panel the interaction effect was not significant. *, $p < 0.05$; significant difference between the groups at the indicated time point (Bonferroni's multiple comparisons posttest). Data for individual sexes can be found in Supplemental Fig. 5.